ELSEVIER

Journal of Nuclear Materials 266–269 (1999) 446–451

journal of nuclear materials

Impurity screening in the RFX reversed field pinch

L. Carraro *, M.E. Puiatti, F. Sattin, P. Scarin, M. Valisa, G. DePol, R. Pasqualotto, R. Pugno, G. Telesca

Consorzio RFX, Corso Stati, Uniti 4, 35127 Padova, Italy

Abstract

Despite the large input power of tens of MW, in the reversed field pinch RFX, the effective charge can be remarkably small. Z_{eff} decreases with density but does not show a dependence on the plasma current up to 1 MA for a given density. It is found that due to the large total particle outflux (2×10^{23} s^{-1}) the energy per particle is kept within reasonable levels. These values, together with the carbon yield and ultimately the impurity concentrations, are comparable with the tokamak case, where typically both power input and particle outflux are proportionally lower by an order of magnitude. Experimental results and Monte Carlo simulations suggest that in RFX the particle screening is due to the short ionisation length of neutrals with a contribution of the finite Larmor radius effect.

Keywords: RFX; Impurity screening; Monte Carlo simulation

1. Introduction

Reversed field pinch experiments of the present generation can run with plasma currents up to 1 MA and require an ohmic input power of the order of tens of MW to sustain steady-state configurations. Correspondingly the first wall has to withstand relatively large power fluxes. In RFX ($a = 0.46$ m, $R = 2$ m) various sources of asymmetry, such as the radial shift of the plasma column and especially mode-wall locking, cause significant deviations from the ideal situation of an even power distribution onto the armour of graphite tiles and locally the wall loading may exceed the remarkable level of 100 MW m^{-2}. Nevertheless, despite the intense plasma wall interactions, the impurity content in the plasma has always been found to be within acceptable levels, similar to those found in ohmically heated tokamak experiments of similar size, where, however, much less power input is typically involved. Indeed, standard wall conditioning techniques such as boronisation may lead in RFX to an effective charge practically close to one.

In this paper, we try to identify the reasons why the impurity concentration remains low despite the large power dissipated onto the wall. This requires the characterisation of the plasma edge since the impurity penetration depends essentially on the average ionisation length of the sputtered atoms and on the various forces that act on the ionised atoms in the scrape off layer (SOL) or within a few Larmor radii inside the last closed surface.

The discussion is based on several experimental results comprising Z_{eff}, impurity influxes, electron density and temperature evaluations and on the simulations of a Monte Carlo code that describes the carbon behaviour at the edge of an RFP and that in particular has been used to address the question of the relevance of specific processes such as the finite Larmor radius effect, the presence of a radial electric field and of the cross field diffusion.

2. Experimental findings

RFX has so far been operated up to the current of 1 MA with central densities ranging from 1×10^{19} to 1×10^{20} m^{-3}. The average Z_{eff}, measured from the

* Corresponding author. Tel.: +39 49 829 5032; fax: +39 49 870 0718; e-mail: spectroscopy@igi.pd.cnr.it.

0022-3115/99/$ – see front matter
PII: S0022-3115(98)00827-7

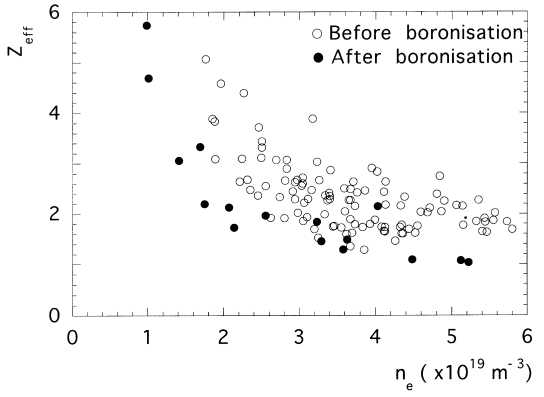

Fig. 1. Plasma effective charge dependence on electron density before and after a boronisation procedure. The data refer to discharges with 500 kA $\leqslant I_p \leqslant$ 600 kA.

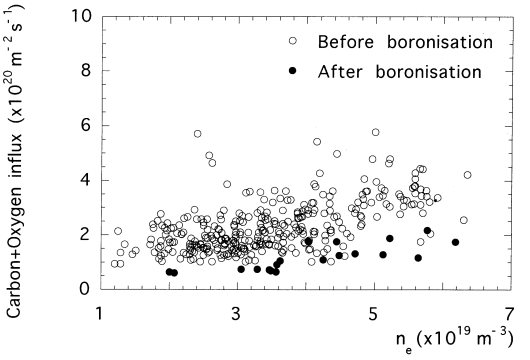

Fig. 3. Impurity influx as a function of the average electron density; the reduction corresponding to a boronisation conditioning procedure is shown. The applied ionisation events per photon correspond to the electron temperature and density values observed by means of a thermal helium beam.

continuum emission at 523.5 ± 0.5 nm, shows a dependence on the electron density as indicated in Fig. 1, that compares the effective charge values in 600 kA discharges before and after a boronisation procedure. After boronisation Z_{eff} decreases at all densities and reaches values even below ≈1.5. The spread of the data at a given density is beyond the estimated error, of the order of 20% [1], and may be ascribed to differences in the conditioning level of the first wall as well as to differences in the main edge parameters.

Z_{eff} does not seem to depend significantly on the plasma current. This finding, shown in Fig. 2 for a data ensemble with the same density, is apparently in contrast with the typical tokamak situation where Z_{eff} tends to increase with the current level [2].

The influxes of carbon and oxygen, measured by means of interference filters centred around C II and O II lines [3] and by applying the ionisation events per photon from [4], increase with density as shown in Fig. 3 for the same shots of Fig. 1. Each point is the average of the measurements along five lines of sight that intercept the wall at different poloidal angles to take into account the asymmetry associated with the radial shift of the plasma column [3]. To evaluate the ionisation events per photon, we have used the electron temperatures and densities measured from the line emission of a helium thermal beam injected on the equatorial plane and on the outboard side of the torus. With the present geometry the results of this technique [5] represent an average between 0.5 and 1 cm from the wall. Fig. 4 illustrates the n_e and T_e measurements as a function of the central electron density. While the edge density increases linearly by a factor 3, the edge temperature only reduces from 75 to 45 eV.

The hydrogen influx measured from the H_α line [6] appears to have a weaker dependence on density (Fig. 5). There is, however, a source of uncertainty in this analysis that comes from the possibility of

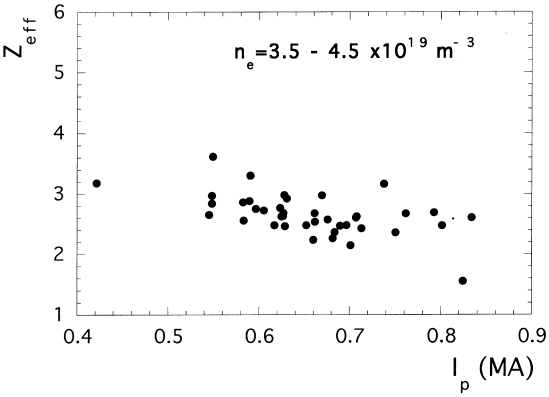

Fig. 2. Plasma effective charge behaviour as a function of the plasma current for a selected range of the average electron density 3.5×10^{19} m$^{-3} \leqslant n_e \leqslant 4.5 \times 10^{19}$ m^{-3}.

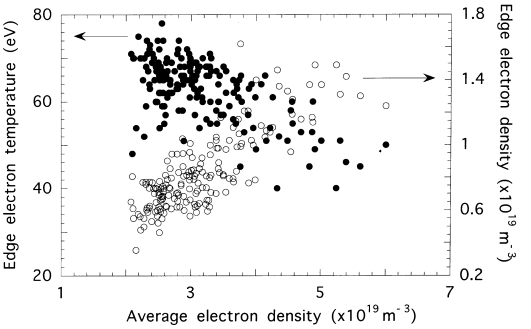

Fig. 4. Edge electron temperature and density measured from the line emission of a thermal helium beam as a function of the average electron density from a CO_2 interferometer.

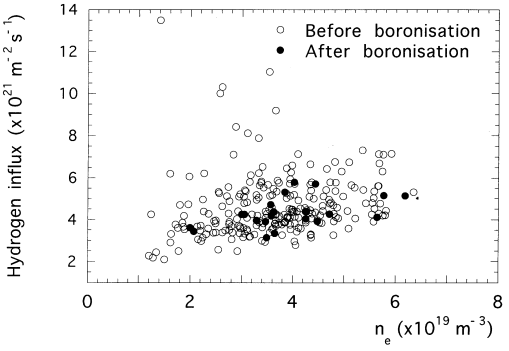

Fig. 5. Hydrogen influx as a function of the average electron density measured before and after a boronisation procedure.

important molecular release, a fraction of which can be ionised without stepping through the atomic state [7]. Therefore measurements from H_α are likely to underestimate the actual hydrogen influx. Besides, the degree of imprecision of the hydrogen influx from H_α could depend on density since the ratio of the ionisation events per photon for molecules to the one for atoms increases with the density above $5-6 \times 10^{18}$ m^{-3} [8].

Also the amount of eroded carbon associated to the molecular input of higher hydrocarbons and methane deduced, respectively, from the C_2 band at 516 nm and from the CH band at 430 nm, may be significant, doubling the carbon influx deduced from the first ionisation level (the database of the molecular emission is insufficient to analyse a possible dependence on the electron density). Chemical sputtering seems therefore to be a relevant production mechanism. The ion temperatures deduced from the Doppler broadening of C III corroborate the latter statement. In fact, they vary between 40 and 50 eV at $n_e = 2 \times 10^{19}$ m^{-3} to 20 eV at $n_e = 6 \times 10^{19}$ m^{-3}, i.e. in a range where the physical sputtering yield, comprised self-sputtering, is relatively low [9].

Finally it should be mentioned that metals have only seldom appeared in the RFX spectra, despite evidence of strong erosion of the inconel vessel especially in the regions affected by large field errors, such as the poloidal gaps on the external conducting shell. Evidence of metal redeposition was, on the other hand, found on the back of the carbon tiles in the same regions [10] meaning that the tile configuration is generally successful in trapping the atoms sputtered at the vessel, in conjunction with the relatively large Larmor radius of metals and their short ionisation length.

3. Monte Carlo simulations

Simulations of the carbon behaviour at the edge of an RFP have been carried out by means of a two-dimensional Monte Carlo code in order to analyse the impact on the screening process of the relevant parameters such as $T_e(r)$, $n_e(r)$, the cross field diffusion D, the Larmor radius, a radial electric field and the energy of the incoming atom.

The code computes the spatial distribution of the low ionisation states of the carbon impurity. The radial T_e and n_e profiles are assumed according to the experimental estimates and are fitted with a power law $\propto 1 - (r/a)^\alpha$, with $\alpha = 30$ for n_e and 4 for T_e. The plasma is assumed to be toroidally symmetric and a uniform horizontal shift of the plasma column is taken into account. The associated SOL is modelled through an exponential decay of temperature and density with an e-folding length of 2 cm, according to the indications of the Langmuir probes.

The motion of the particle is computed from the forces acting on it without resorting to the guiding center approximation; the forces included in the model comprise the Lorentz force, the radial electric force, the pressure gradient force, all given in input. Besides, the diffusion is modelled as a random shift of the particle position. Finally the charge of the particle is modified by ionisation and/or recombination, modelled as probabilistic processes with frequency determined by the local plasma properties.

A radial electric field (inward at the edge and outward in the plasma core) has been introduced reproducing the experimental value measured by edge probes [11]. The experimental shear has been approximated by a simple linear function varying from -3 kV/m at the wall to +3 kV/m at a radius r_0 in the plasma. r_0 is 2 cm from the wall for 500 kA discharges.

The penetration efficiency ξ is defined as the fraction of the injected particles that enter the plasma by a few centimetres. In the present simulations we have placed this threshold at 4.5 cm from the wall, that corresponds to several Larmor radii for C II in a variety of plasma edge situations. While the arbitrariness of the definition affects the absolute results, the trends against the various parameters are preserved until the scale length of the considered processes do not vary too much with respect to the defined distance. In particular, the choice allows the comparison of particles with relatively large Larmor radius – either due to a low magnetic field or to a large entrance velocity – that intercept the wall after an excursion of a few cms into the plasma. It is worth noticing that for typical RFX edge conditions ($T_e = 50$ eV, $n_e = 1 \times 10^{19}$ m^{-3}, $B_{pol} = 0.3$ T) the ionisation frequency of C II is $\approx 1.2 \times 10^5$ s^{-1}, that is smaller than its gyrofrequency $\approx 3.8 \times 10^5$ s^{-1}.

The number of particles injected for each simulation has been chosen so as to limit statistical fluctuations within a few percent, ranging from 3000 to 12,000.

The role of relevant parameters on the screening has been studied by varying each of them individually in a simplified arrangement: by injecting monoenergetical

particles radially from the wall on the equatorial plane and following them along their trajectory until their loss onto the wall or their penetration beyond the threshold into the plasma and neglecting self-sputtering. The main results are reported in Table 1 and are summarised in the following:

1. The penetration efficiency (ξ) is practically independent of the Larmor radius when varying only the magnetic field beyond 0.2 T.
2. ξ is a strongly increasing function of the input velocity, varying from 10% for energies typical of chemical sputtering (0.25 eV) to 31% for pure physical sputtering (10 eV).
3. ξ is, as expected, dependent upon the edge values and the profiles of temperature and density, since their increase keeps the particles closer to the last closed plasma surface.
4. The effect of a radial electric field negative at the wall (inward) and positive inside (outward), as experimentally found, reduces the penetration probability.
5. The cross field diffusion, modelled as a random shift of the particle position, is practically ineffective.

A result not reported in Table 1 is that the redeposition length along the poloidal direction has a characteristic value of 10–15 cm in agreement with the results of an inspection on the machine and the analysis of sample probes [10].

More realistic simulations, including self-sputtering and chemical sputtering [12] from the whole poloidal circumference with angular and energetic distribution, yield a screening efficiency a factor of 2 larger than the reference case of Table 1. This may be explained in terms of a shorter effective ionisation length related to the lower average radial entrance velocity. The results of these simulations have been compared with the radial emissivity profiles of C I, C II lines monitored by a CCD camera looking tangentially at the inboard wall [13]. Fig. 6 shows the result of such a comparison for shots with 600 kA and central density around 3×10^{19} m^{-3} and a radial plasma shift of 1 cm.

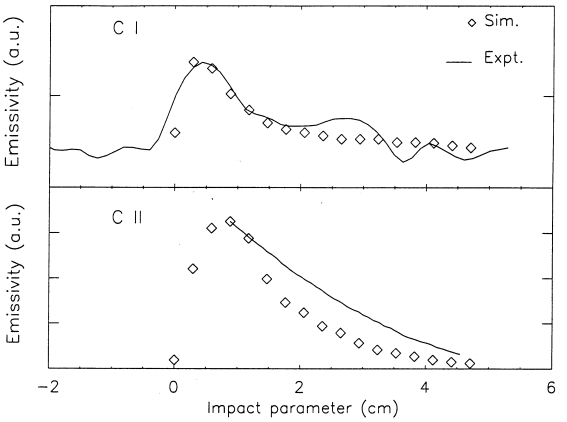

Fig. 6. Comparison between the radial C I and C II emissivity profiles measured by a CCD camera looking tangentially at the inboard wall and the Monte Carlo simulation.

Table 1
Results of the Monte Carlo simulations for particles injected from the outboard side of the torus

#run	Notes	ξ (%)	λ_{ion} C I (cm)	C II losses (%)	C III losses (%)	C IV losses (%)
1	$B = 0.3$ T $D = 10$ m^2/s $T_e(r=a) = 15$ eV $n_e(r=a) = 3 \times 10^{18}$ m^{-3} $E_{sputtering} = 1$ eV	14	0.7	43	27	16
2	$B = 0.8$ T	15	0.7	44	24	17
3	$B = 0.5$ T	16	0.7	44	25	15
4	$B = 0.1$ T	22	0.7	29	30	19
5	$n_e(r=a) = 1 \times 10^{18}$ m^{-3}	31	1.3	34	25	10
6	$n_e(r=a) = 9 \times 10^{18}$ m^{-3}	10	0.4	50	26	14
7	$n_e(r=a) = 1.2 \times 10^{19}$ m^{-3}	9	0.4	50	27	14
8	$T_e(r=a) = 45$ eV	8	0.4	48	28	16
9	$T_e(r=a) = 60$ eV	7	0.4	51	26	16
10	$D = 1$ m^2/s	13	0.7	30	27	29
11	$D = 100$ m^2/s	17	0.7	63	16	4
12	$E_{sputtering} = 10$ eV	31	1.3	22	23	24
13	$E_{sputtering} = 0.25$ eV	10	0.4	59	20	11
14	Electric field, shear (shear = 300 kV/m^2)	7	0.7	31	30	32

ξ is the fraction of particles that overcome the threshold of 4.5 cm inside the plasma, λ_{ion} is the ionisation length of C I. The fraction of losses onto the wall is distinguished according to the ionisation state up to C IV.

4. Discussion

In a simplified approach to the problem of the impurity contamination, the impurity concentrations may be expressed as a function of the product of the ratio between the impurity and the hydrogen influxes, their particle confinement times (τ_{imp},τ_H) and their penetration probabilities

$$(\xi_{imp},\xi_H): Z_{eff} \propto \frac{n_{imp}}{n_e} \propto \frac{\Gamma_{imp}}{\Gamma_H}\frac{\tau_{imp}}{\tau_H}\frac{\xi_{imp}}{\xi_H}.$$

In the comparison between RFX and ohmically heated tokamaks with carbon-facing components, it is interesting to notice that, for the same density ranges, the so-called carbon yield Γ_C/Γ_H is comparable and around 0.01–0.04 [14]. Fluctuations in the carbon yield, even within the same experiment, may be ascribed to various reasons, comprised of the oxygen contribution, the conditioning level and the surface temperatures of the tiles, changes in the edge parameters as well as to the uncertainties in the determinations of both carbon and hydrogen influxes.

Little is known about the particle confinement time in RFPs as a function of the mass and charge. For hydrogen it has been found that the core region is dominated by magnetic stochasticity while in the region outside the reversal radius hydrogen flux is consistent with the transport due to electrostatic fluctuations [15]. On this basis, we deem it unlikely that impurities are confined less than hydrogen. If we assume that τ_{imp}/τ_H is of the order unity as in an L-mode tokamak [16], the analogy of the plasma contamination suggests that ξ_{imp}/ξ_H is similar in value for tokamaks and RFPs, despite the widely different scheme of particle disposal. Indeed while in a tokamak, screening of the ionised impurities takes place in the SOL due to the electric field and drag force acting along the open field lines, in RFX all neutrals are likely to be ionised directly in the confined plasma.

The similarities in the contamination level found in devices that differ in magnetic configuration and, by order of magnitudes, in confinement properties would indicate that confinement itself is not playing a dominant role in determining the effective charge of the plasma. Z_{eff} appears instead to be regulated by a number of detailed processes at the edge that determine the impurity production and its screening.

The results described above suggest that in RFX the main screening effect is to be ascribed to the relatively short ionisation length associated to the edge and temperature values and to the relevant contribution of chemical sputtering. Both Monte Carlo simulations and the experimental observations of molecular and atomic influxes agree in assigning a share of $\approx$50% to the two main sputtering mechanisms. Besides, a reduced ionisation length increases the losses due to the finite Larmor radius. This is seen in Table 1, where the increase of T_e and n_e increases the C II losses at the expense of the fraction of the penetrating particles.

An independent increase of the Larmor radius is instead more subtle in its effects since particles are allowed to move deeper into the plasma where the competing action of ionisation may take over. This is seen for instance in Table 1 for the case with reduced B, where the penetration increases and the C II losses decrease.

Finally, the presence of a radial electric field such as that experimentally found, seems to introduce in RFX a significant effect on the plasma contamination, opposite to the impurity penetration.

5. Conclusions

Recalling the original issue about the reasons why in RFX the impurity concentration remains low despite the large power dissipated onto the wall, one observes that the large input power is accompanied by a large particle outflux in such a way that the energy per particle is kept within reasonable levels. In fact the ratio of the power input to the total particle outflux $\Phi_{E_{out}}/\Gamma_{out}$ ($\approx$20 MW/2×10^{23} s^{-1} for RFX) is comparable with the tokamak case, where typically both power input and particle outflux are proportionally lower by an order of magnitude. This leads to similar carbon yield for the contribution of physical sputtering and ultimately to comparable contamination levels in the two configurations, although the detailed screening processes might present some differences. In RFX, the reduction of Z_{eff} with increasing plasma density is due to the shortening of the ionisation length that, with an increasing contribution of the finite Larmor radius effect, increases the screening; in a tokamak it is due to the increased drag on the impurities in the SOL [17]. The screening increase with T_e obtained from the Monte Carlo simulation is due both to a reduced ionisation length and increased Larmor radius of thermalized impurities. On the contrary, in a tokamak increasing the SOL temperature reduces the drag and reduces the screening [17]. This may explain the different behaviour of Z_{eff} with plasma current in the two configurations.

A more refined analysis of the plasma contamination in RFX and of its comparison with the tokamak case, requires that detailed experiments be addressed to the comprehension of the impurity production and of the transport of the impurities at the edge, for instance with ad hoc impurity injections.

Acknowledgements

Enlightening discussions with Dr R. Bartiromo are gratefully acknowledged.

References

[1] L. Carraro, M.E. Puiatti, F. Sattin et al., in: Proceedings of the 24th Conference on Plasma Physics and Controlled Fusion, Berchtesgaden, 9–13 June, vol. I, 1997, p. 329.
[2] K. Behringer et al., J. Nucl. Mater. 162–164 (1989) 398.
[3] L. Carraro, E. Casarotto, R. Pasqualotto et al., J. Nucl. Mater. 220–222 (1995) 646.
[4] K. Behringer et al., Plasma Phys. Contr. Fusion 31 (1989) 2059.
[5] M. Brix, B. Schweer, in: Proceedings of the 24th Conference on Plasma Physics and Controlled Fusion, Berchtesgaden, 9–13 June 1997, vol. IV, p. 1837.
[6] L.C. Johnson, E. Hinnov, J. Quant. Spectr. and Rad. Transf. 13 (1973) 33.
[7] A. Pospieszczyk, G. Sergienko, D. Rusbüld et al., in: Proceedings of the 24th Conference on Plasma Physics and Controlled Fusion, Berchtesgaden, 9–13 June, vol. IV, p. 1733.
[8] K. Sawada, K. Eriguchi, T. Fujimoto, J. Appl. Phys. 73 (1993) 812.
[9] J. Roth, J. Nucl. Mater. 176&177 (1990) 132.
[10] V. Antoni, M. Bagatin, H. Bergsåker et al., J. Nucl. Mater. 220–222 (1995) 650.
[11] V. Antoni, D. Desideri, E. Martines et al., Phys Rev. Lett. 79 (1997) 4814.
[12] R.K. Janev, Atomic and Plasma-Material Interaction Data for Fusion, vol. 1, IAEA, Vienna, 1991; J. Roth et al., Nucl. Fusion 36 (1996) 1647.
[13] R. Pasqualotto, R. Pugno, M. Valisa et al., Plasma Dev. Op. 5 (1998) 287.
[14] H.G. Esser et al., J. Nucl. Mater. 220–222 (1995) 457; A.R. Field et al., J. Nucl. Mater. 220–222 (1995) 553; Matthews et al., J. Nucl. Mater. 196–198 (1992) 374; H. Kubo et al., J. Nucl. Mater. 196–198 (1992) 71.
[15] D. Gregoratto, L. Garzotti et al., Nucl. Fusion, 38 (1998) 1199; V. Antoni et al., Phys. Rev. Lett. 80 (1998) 4185.
[16] G. Fussmann, A.R. Field, A. Kallembach et al., Plasma Phys. Contr. Fusion 33 (1991) 1677.
[17] R. Bartiromo, I. Condrea, R. De Angelis et al., Nucl. Fusion 35 (1995) 1161.